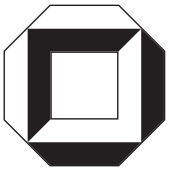

UNIVERSITÄT KARLSRUHE

Optimality Of The Fully Discrete Filtered Backprojection Algorithm For Tomographic Inversion

A. Rieder
A. Schneck

Preprint Nr. 06/09

Institut für Wissenschaftliches Rechnen
und Mathematische Modellbildung

76128 Karlsruhe

Anschriften der Verfasser:

Prof. Dr. Andreas Rieder
Institut für Angewandte und Numerische Mathematik und Institut für Wissenschaftliches Rechnen und Mathematische Modellbildung
Universität Karlsruhe
D-76128 Karlsruhe

Arne Schneck
Graduiertenkolleg 1294: Analysis, Simulation und Design nanotechnologischer Prozesse
Universität Karlsruhe
D-76128 Karlsruhe

OPTIMALITY OF THE FULLY DISCRETE FILTERED BACKPROJECTION ALGORITHM FOR TOMOGRAPHIC INVERSION

ANDREAS RIEDER† AND ARNE SCHNECK‡

Abstract. Although the filtered backprojection algorithm (FBA) has been the standard reconstruction algorithm in 2D computerized tomography for more than 30 years, its convergence behavior is not completely settled so far. Relying on convergence results by Rieder and Faridani for the semi-discrete FBA [*SIAM J. Numer. Anal., 41(3), 869-892, 2003*] we show optimality of the fully discrete version and of a related algorithm.

Key words. 2D-Radon transform, tomography, parallel scanning geometry, filtered backprojection algorithm, reconstruction filter, optimality.

AMS subject classifications. 65R20.

1. Introduction. X-Ray computerized tomography (CT) is a technique for imaging the density distribution inside an object. Mathematically speaking, CT reduces to reconstructing a function from its integrals along straight lines, see, e.g., Natterer [8] for details.

The mathematical model in 2D is the *Radon transform*

$$\mathbf{R}f(s,\vartheta) := \int_{L(s,\vartheta)} f(x)\ \mathrm{d}\sigma(x),$$

mapping a function to its integrals over the lines $L(s,\vartheta) = \{\tau\,\omega^{\perp}(\vartheta) + s\,\omega(\vartheta)\,|\,\tau\in\mathbb{R}\}$ where $s\in\mathbb{R}$, $\omega(\vartheta) = (\cos\vartheta, \sin\vartheta)^t$, and $\omega^{\perp}(\vartheta) = (-\sin\vartheta, \cos\vartheta)^t$ for $\vartheta\in[0,\pi]$. We assume throughout that the searched-for density distributions are compactly supported in Ω, the unit disk in $\mathbb{R}^2$ centered about the origin. Thus, the lateral variable s may be restricted to $[-1,1]$.

In the *parallel scanning geometry* we observe the discrete Radon data

$$D = \{\mathbf{R}f(kh, jh_\vartheta) : k = -q,\dots,q,\ j = 0,\dots,p-1\},\quad p,q\in\mathbb{N}, \tag{1.1}$$

where $h = 1/q$ is the lateral sampling rate and $h_\vartheta = \pi/p$ is the angular sampling rate. Let $f_{\mathrm{FBA}} = f_{\mathrm{FBA}}(h,h_\vartheta)$ denote the reconstruction of f by the filtered backprojection algorithm (FBA) from D. Then, we will show

†Institut für Angewandte und Numerische Mathematik and Institut für Wissenschaftliches Rechnen und Mathematische Modellbildung, Universität Karlsruhe, 76128 Karlsruhe, Germany, URL: `www.mathematik.uni-karlsruhe.de/prakmath/~rieder`, email: `andreas.rieder@math.uni-karlsruhe.de`

‡Graduiertenkolleg 1294 "Analysis, Simulation and Design of Nanotechnological Processes", Fakultät für Mathematik, Universität Karlsruhe, 76128 Karlsruhe, Germany, email: `aschneck@gmx.de`

that*

$$\begin{aligned}&\|f - f_{\mathrm{FBA}}\|_{L^2(\Omega)}\\ &\quad\lesssim \big(h^{\min\{\alpha_{\max},\alpha\}} + h_\vartheta^\alpha + h_\vartheta h^{\min\{\alpha_{\max},\alpha-1\}}\big)\|f\|_{H_0^\alpha(\Omega)}, \quad \alpha \geq 1.\end{aligned} \tag{1.2}$$

The maximal lateral convergence rate $\alpha_{\max}$ depends on the used filter and the interpolation process after filtering. For instance,

$$\alpha_{\max} = \begin{cases} 3/2 & \text{Shepp-Logan filter with piecewise constant interpolation,}\\ 2 & \text{Shepp-Logan filter with piecewise linear interpolation,}\\ 5/2 & \text{mod. Shepp-Logan filter with piecewise linear interpolation.}\end{cases} \tag{1.3}$$

In principle, it is possible to construct filters and adapted local interpolation schemes leading to arbitrarily large $\alpha_{\max}$.

Moreover, we introduce algorithm MFBA, a modification of FBA, and we prove that

$$\begin{aligned}&\|f - f_{\mathrm{MFBA}}\|_{L^2(\Omega)}\\ &\qquad\lesssim (h^{\min\{\alpha_{\max},\alpha\}} + h_\vartheta^{\min\{5/2-\epsilon,\alpha\}})\,\|f\|_{H_0^\alpha(\Omega)}, \quad \alpha > 1/2,\end{aligned} \tag{1.4}$$

for any $\epsilon > 0$ where $\alpha_{\max}$ is as in (1.3).

The paper is organized as follows. In the next section we introduce the filtered backprojection algorithm, recall the convergence result of Rieder and Faridani [9], and give some stability estimates for the Radon transform which we will need later. Then we present and prove our convergence estimate for the fully discrete FBA in Section 3. Section 4 is devoted to our modified filtered backprojection algorithm: We motivate its definition, prove convergence, and discuss some aspects of its implementation. Numerical experiments visualize our convergence results of both algorithms in the final section where also a qualitative comparison is presented.

2. The filtered backprojection algorithm. In this section we introduce the FBA in detail and recall results which we will need later.

First, we present some notation. Let $\widehat{f}(\xi) := (2\pi)^{-d/2}\int_{\mathbb{R}^d} f(x)\,\mathrm{e}^{-\imath\,\xi^t x}\,\mathrm{d}x$ denote the Fourier transform of a function f in $L^1(\mathbb{R}^d)\cap L^2(\mathbb{R}^d)$. The Fourier transform can be extended to L^2-functions and tempered distributions by continuity and duality. We define the Sobolev spaces $H^\alpha(\mathbb{R}^d)$, $\alpha\in\mathbb{R}$, to be the closure of the Schwartz class with respect to the norm

$$\|f\|_\alpha^2 := \int_{\mathbb{R}^d} \big(1+|\xi|^2\big)^\alpha\,|\widehat{f}(\xi)|^2\,\mathrm{d}\xi.$$

*$A \lesssim B$ indicates the existence of a generic constant c such that $A \leq cB$ uniformly in all parameters A and B may depend on.

Starting point for deriving the FBA is the inversion formula

$$f = \frac{1}{4\pi}\mathbf{R}^*(\Lambda \otimes I)\mathbf{R}f$$

which holds true for $f \in L^2(\Omega)$ [9, Sec. 3.2]†. Here, the *backprojection operator*

$$\mathbf{R}^* g(x) = \int_0^{2\pi} g(x^t\omega(\vartheta), \vartheta)\,\mathrm{d}\vartheta \tag{2.1}$$

is the adjoint of $\mathbf{R} \in \mathcal{L}\big(L^2(\Omega), L^2(Z)\big)$ with $Z = [-1,1] \times [0,2\pi]$. The Λ-operator is defined by

$$\widehat{\Lambda u}(\xi) = |\xi|\widehat{u}(\xi)$$

and maps $H^\alpha(\mathbb{R}^d)$ boundedly to $H^{\alpha-1}(\mathbb{R}^d)$. The binary operation $\otimes$ denotes the tensor product of operators and spaces, respectively, see, e.g., Aubin [1]. Therefore, Λ in $(\Lambda\otimes I)\mathbf{R}f$ only affects the lateral variable (I is the identity).

Due to Rieder and Faridani [9] FBA can be written as

$$f_{\mathrm{FBA}}(x) := \mathbf{R}^*_{h_\vartheta}(\mathrm{I}_h\Lambda E_h \otimes I)\mathbf{R}f(x) \tag{2.2}$$

where

$$\mathbf{R}^*_{h_\vartheta} g(x) := h_\vartheta \sum_{j=0}^{2p-1} g(x^t\omega(\vartheta_j), \vartheta_j), \quad \vartheta_j = jh_\vartheta.$$

The operators E_h and I_h are generalized interpolation operators: For $u \in H^\alpha(\mathbb{R})$ define

$$E_h u(s) := h^{-1} \sum_{k\in\mathbb{Z}} \big\langle u, \epsilon_h(\cdot - s_k)\big\rangle\, B_h(s - s_k) \tag{2.3}$$

where $\epsilon_h(s) = \epsilon(s/h)$ and $B_h(s) = B(s/h)$. Here, $B \in L^2(\mathbb{R})$ is the 'interpolation function' and $\epsilon \in H^{-\alpha}(\mathbb{R})$ is assumed to be even with $\widehat{\epsilon}(0) = 1/\sqrt{2\pi}$. Further, $\langle\cdot,\cdot\rangle$ denotes the duality pairing in $H^\alpha(\mathbb{R}) \times H^{-\alpha}(\mathbb{R})$. For $u \in H^\alpha(\mathbb{R})$, $\alpha > 1/2$, we may choose $\epsilon = \delta$ (Dirac distribution). In this case, $h^{-1}\langle u, \epsilon_h(\cdot - s_k)\rangle = u(s_k)$. Analogously,

$$\mathrm{I}_h u(s) := h^{-1} \sum_{k\in\mathbb{Z}} \big\langle u, \eta_h(\cdot - s_k)\big\rangle\, A_h(s - s_k), \tag{2.4}$$

where η and A play the roles of ϵ and B, respectively. For more details on E_h and I_h we refer to [9, Sec. 3.2].

Observe that

$$(\mathrm{I}_h\Lambda E_h\otimes I)\mathbf{R}f(s,\vartheta) = \sum_{\ell\in\mathbb{Z}} \Big(\sum_{k\in\mathbb{Z}} w_{\ell-k}\big\langle \mathbf{R}f(\cdot,\vartheta), \epsilon_h(\cdot - s_k)\big\rangle\Big) A_h(s - s_\ell), \tag{2.5}$$

†Later in the paper we will benefit from the 2π-periodicity of $\mathbf{R}f(s,\cdot)$. Therefore, the angular variable from now on runs in the interval $[0,2\pi]$. From a practical point of view, however, it suffices to know $\mathbf{R}f$ on $[-1,1]\times[0,\pi]$ to recover f.

with $w_r = \upsilon(r)/h^2$ where

$$\upsilon(s) := \frac{1}{\pi} \int_0^\infty \sigma\, \widehat{B}(\sigma)\, \widehat{\eta}(\sigma) \cos(s\sigma) \mathrm{d}\sigma$$

is the *reconstruction filter*. Thus, the evaluation of $f_{\mathrm{FBA}}(x)$ can be implemented exactly as in [8, Chap. V.1.1]. The sum over k in (2.5) represents the filtering step.

We require the following approximation properties of E_h and I_h, respectively:

(i) There are non-negative constants $\tau_{\max}$ and $\beta_{\min} \le \beta_{\max}$ such that

$$\|E_h u - u\|_\tau \lesssim h^{\beta-\tau} \|u\|_\beta \tag{2.6}$$

for $\beta_{\min} \le \beta \le \beta_{\max}$, $1/2 \le \tau \le \tau_{\max}$, $\tau \le \beta$ and any $u \in H_0^\beta(-1,1)$[‡].

(ii) There is a constant $\alpha_{\mathrm{I}} > 0$ such that

$$\|\mathrm{I}_h - I\|_{H^{\alpha-1/2}(\mathbb{R}) \to H^{-1/2}(\mathbb{R})} \lesssim h^\alpha \tag{2.7}$$

for $0 \le \alpha \le \alpha_{\mathrm{I}}$.

Both estimates, (2.6) and (2.7), are meant asymptotically as $h \to 0$. All further estimates involving h or h_ϑ have to be understood in similar manner.

Rieder and Faridani studied a semi-discrete version of FBA, that is, they did not consider discretization of the angular variable. Their result [9, Th. 3.7] is formulated in the following theorem (Natterer [6] gave a convergence result for the other semi-discrete version of FBA where the angular variable is discretized but not the lateral).

THEOREM 2.1. *Under* (2.6) *and* (2.7) *with* $\beta_{\max}, \tau_{\max} \ge 1/2$ *we have that*

$$\big\| f - \frac{1}{4\pi} \mathbf{R}^* (\mathrm{I}_h \Lambda E_h \otimes I) \mathbf{R} f \big\|_{L^2(\Omega)} \lesssim h^\alpha \|f\|_\alpha$$

for $\max\{0, \beta_{\min} - 1/2\} \le \alpha \le \min\{\alpha_{\mathrm{I}}, \beta_{\max} - 1/2, \tau_{\max} - 1/2\}$ *and* $f \in H_0^\alpha(\Omega)$.

We present concrete examples; for proofs see again [9]. Set

$$\widetilde{f}_{\mathrm{FBA}} = \frac{1}{4\pi} \mathbf{R}^* (\mathrm{I}_h \Lambda E_h \otimes I) \mathbf{R} f.$$

EXAMPLE 2.2 (Shepp-Logan filter with nearest-neighbor interpolation). *Let* $B(\cdot) = \mathrm{sinc}(\pi\,\cdot)$[§] *be the interpolating function in* E_h *and* $A = \mathbf{1}_{[-1/2,1/2]}$[¶]

[‡] $H_0^\alpha(D)$ is the closure of $\mathcal{C}_0^\infty(D)$, the space of infinitely differentiable functions compactly supported in $D \subset \mathbb{R}^d$, with respect to the norm $\|\cdot\|_\alpha$.

[§] sinc is the *sinus cardinals*: $\mathrm{sinc}(s) = (\sin s)/s$.

[¶] $\mathbf{1}_D$ denotes the indicator function of D.

the interpolating function in I_h. *Further, let* $\eta = \mathbf{1}_{[-1/2,1/2]}$ *in* I_h. *Then, the discrete filter* $\{w_r\}_{r\in\mathbb{Z}}$ *in* (2.5) *is the Shepp-Logan filter* [12]*:*

$$w_r = \frac{2}{\pi^2\, h^2}\ \frac{1}{1-4\,r^2}. \tag{2.8}$$

Further,

$$\big\|\widetilde{f}_{\mathrm{FBA}} - f\big\|_{L^2(\Omega)} \lesssim h^{\min\{3/2,\,\alpha\}}\,\|f\|_\alpha \quad \textit{for } f\in H_0^\alpha(\Omega),\ \alpha>0,$$

as long as ϵ *in* E_h *is either an even, compactly supported and normalized* L^2*-function or the Dirac distribution.*

Example 2.3 (Shepp-Logan filter with piecewise linear interpolation). *Let* E_h *and* I_h *be as in Example* 2.2*, except for* A *which is now the linear B-spline, that is,* $A = \mathbf{1}_{[-1/2,1/2]} \star \mathbf{1}_{[-1/2,1/2]}$. *Hence,* I_h *interpolates piecewise linear. The discrete filter* $\{w_r\}_{r\in\mathbb{Z}}$ *is as in* (2.8). *Here, we have*

$$\big\|\widetilde{f}_{\mathrm{FBA}} - f\big\|_{L^2(\Omega)} \lesssim h^{\min\{2,\,\alpha\}}\,\|f\|_\alpha \quad \textit{for } f\in H_0^\alpha(\Omega),\ \alpha>0.$$

Example 2.4 (modified Shepp-Logan filter with piecewise linear interpolation). *Let* E_h *and* I_h *be as in Example* 2.3*, except for* η *which is now given by*

$$\widehat{\eta}(\sigma) = (2\pi)^{-1/2}\frac{\operatorname{sinc}(\sigma/2)}{3/4+\cos(\sigma)/4}.$$

The corresponding discrete filter $\{w_r\}_{r\in\mathbb{Z}}$ *is called modified Shepp-Logan filter* [9]. *Here,*

$$\big\|\widetilde{f}_{\mathrm{FBA}} - f\big\|_{L^2(\Omega)} \lesssim h^{\min\{5/2,\,\alpha\}}\,\|f\|_\alpha \quad \textit{for } f\in H_0^\alpha(\Omega),\ \alpha>0.$$

For later use we compile Sobolev space estimates of the Radon transform. Set $H^{(\alpha,\beta)} := H^\alpha(\mathbb{R})\otimes H^\beta_{\mathrm{p}}(0,2\pi)^{\|}$. Due to Natterer and Louis [5] we have

$$\|\mathbf{R}f\|_{H^{(\alpha+1/2,0)}} \lesssim \|f\|_\alpha \ \text{ for any } f\in H_0^\alpha(\Omega),\ \alpha\ge 0.$$

A similar continuity estimate by Rieder and Schuster [10] yields especially

$$\|\mathbf{R}f\|_{H^{(0,\alpha+1/2)}} \lesssim \|f\|_\alpha \ \text{ for any } f\in H_0^\alpha(\Omega),\ \alpha\ge 0.$$

Interpolating both latter mapping properties of $\mathbf{R}$ finally results in

$$\|\mathbf{R}f\|_{H^{(\beta,\alpha+1/2-\beta)}} \lesssim \|f\|_\alpha \text{ for any } 0\le\beta\le\alpha+1/2-\beta \tag{2.9}$$

and $f\in H_0^\alpha(\Omega)$.

$^{\|}$For the definition of the Sobolev spaces $H^\beta_{\mathrm{p}}(a,b)$ of periodic functions with period $b-a$, see, for instance, Lions and Magenes [4, Chap. 1.7].

3. Convergence of the fully discrete FBA. In this section we will prove our asymptotic convergence estimate of FBA which is stated in the following theorem.

THEOREM 3.1. *Under* (2.6) *and* (2.7) *with* $\beta_{\max}, \tau_{\max} \geq 3/2$ *we have that*

$$\begin{aligned}\big\|f - \frac{1}{4\pi}\mathbf{R}_{h\vartheta}^*(\mathrm{I}_h\Lambda E_h \otimes I)\mathbf{R}f\big\|_{L^2(\Omega)} \\ \lesssim \big(h^{\min\{\alpha_{\max},\alpha\}} + h_\vartheta^\alpha + h_\vartheta h^{\min\{\alpha_{\max},\alpha-1\}}\big)\|f\|_\alpha, \quad \alpha \geq \alpha_{\min},\end{aligned}$$

where $\alpha_{\min} = \max\{1, \beta_{\min} - 1/2\}$, $\alpha_{\max} = \min\{\alpha_{\mathrm{I}}, \beta_{\max} - 1/2, \tau_{\max} - 1/2\}$, *and* $f \in H_0^\alpha(\Omega)$.

The optimal sampling condition $p = \pi q$, see, e.g., Natterer [8, Table III.1], yields the convergence rate h^α as $h \to 0$ which is optimal for density distributions in $H_0^\alpha(\Omega)$, see Natterer [7] or [8, Th. IV.2.2].

Note that Theorem 3.1 reduces to (1.2) with $\alpha_{\max}$ from (1.3) for our concrete settings of Examples 2.2, 2.3, and 2.4.

REMARK 3.2. *In* [9, Remark 4.2] *Rieder and Faridani sketched a scheme to construct interpolation operators* I_h (2.4) *with arbitrarily large* α_{I}. *Further, these interpolation operators are still local since A is a B-spline. Using band-limited interpolation for* E_h, *that is,* $B(\cdot) = \mathrm{sinc}(\pi\,\cdot)$ *and* ϵ *is the Dirac distribution in* (2.3), *we have* $\beta_{\max} = \tau_{\max} = \infty$, *see* [9, Th. B.4]. *Thus, one can construct efficient filtered backprojection schemes with an arbitrarily large* $\alpha_{\max}$. *Of course, one would fully benefit from these highly accurate filtered backprojection schemes if the searched-for density distributions are sufficiently smooth which is not the case in medical imaging but in optical homodyne tomography, see, e.g., Smithey et al.* [13]. *In optical homodyne tomography one determines the Wigner function of the state of a quantum system.*

In the remainder of this section we verify Theorem 3.1. In view of Theorem 2.1 we start with

$$\begin{aligned}\|f - f_{\mathrm{FBA}}\|_{L^2(\Omega)} \leq \big\|f - \frac{1}{4\pi}\mathbf{R}^*(\mathrm{I}_h\Lambda E_h \otimes I)\mathbf{R}f\big\|_{L^2(\Omega)} \\ + \big\|(\mathbf{R}^* - \mathbf{R}_{h\vartheta}^*)(\mathrm{I}_h\Lambda E_h \otimes I)\mathbf{R}f\big\|_{L^2(\Omega)}\end{aligned} \tag{3.1}$$

and it remains to investigate the second error term which involves the discretization of the backprojection operator. We once again apply the triangle

inequality and obtain

$$\begin{aligned}\big\|(\mathbf{R}^* - \mathbf{R}^*_{h_\vartheta})(\mathrm{I}_h \Lambda E_h \otimes I)\mathbf{R}f\big\|_{L^2(\Omega)} \\ \leq \big\|(\mathbf{R}^* - \mathbf{R}^*_{h_\vartheta})\big((\mathrm{I}_h \Lambda E_h - \Lambda) \otimes I\big)\mathbf{R}f\big\|_{L^2(\Omega)} \\ + \big\|(\mathbf{R}^* - \mathbf{R}^*_{h_\vartheta})(\Lambda \otimes I)\mathbf{R}f\big\|_{L^2(\Omega)}.\end{aligned} \tag{3.2}$$

Following we bound each of the norms on the right hand side.

As $\mathbf{R}^*_{h_\vartheta}$ arises from $\mathbf{R}^*$ by applying the composite trapezoidal rule to the integral in (2.1) we will rely on the following estimate for the quadrature error.

LEMMA 3.3. *Let $u \in H^{2k+1}_{\mathrm{p}}(a,b)$ for one $k \in \mathbb{N}_0$. Then,*

$$\Big| \int_a^b u(t)\mathrm{d}t - h \sum_{k=0}^{n-1} u(a+kh) \Big| \lesssim h^{2k+1} \int_a^b |u^{(2k+1)}(t)|\mathrm{d}t$$

where $h = (b-a)/n$ and $n \in \mathbb{N}$.

Proof. Since $\big\{ g|_{[a,b]} : g \in \mathcal{C}^{2k+1}(\mathbb{R}),\ g \text{ is } (b-a)\text{-periodic} \big\}$ is dense in $H^{2k+1}_{\mathrm{p}}(a,b)$ the assertion follows for $k \in \mathbb{N}$ readily from the Euler-Maclaurin formula [3, Cor. 9.27] and the bounded embedding $H^{2k+1}_{\mathrm{p}}(a,b) \hookrightarrow \mathcal{C}([a,b])$. For $k = 0$ the statement may be proved by a straightforward calculation, see, e.g., Schneck [11]. □

LEMMA 3.4. *Let f be in $H^\alpha_0(\Omega)$ for $\alpha \geq 1$. Then,*

$$\big\|(\mathbf{R}^* - \mathbf{R}^*_{h_\vartheta})(\Lambda \otimes I)\mathbf{R}f\big\|_{L^2(\Omega)} \lesssim h_\vartheta^\alpha \, \|f\|_\alpha.$$

Proof. For the time being assume $f \in \mathcal{C}^\infty_0(\Omega)$. We will use a duality argument by Natterer [6]. For $g \in \mathcal{C}^\infty_0(\Omega)$ let

$$u(\vartheta) := \int_\Omega g(x)\Psi(x^t\omega(\vartheta),\vartheta)\,\mathrm{d}x = \int_{-1}^1 \mathbf{R}g(s,\vartheta)\,\Psi(s,\vartheta)\,\mathrm{d}s \tag{3.3}$$

where $\Psi = (\Lambda \otimes I)\mathbf{R}f$. The latter equality follows from the coordinate transformation $x = s\omega(\vartheta) + t\omega^\perp(\vartheta) \mapsto (s,t)$. By a straightforward calculation we find the useful relation

$$|\langle (\mathbf{R}^* - \mathbf{R}^*_{h_\vartheta})\Psi, g\rangle_{L^2}| = \Big| \int_0^{2\pi} u(\vartheta)\,\mathrm{d}\vartheta - h_\vartheta \sum_{j=0}^{2p-1} u(jh_\vartheta) \Big|.$$

Further,

$$\begin{aligned}\big\|(\mathbf{R}^* - \mathbf{R}^*_{h_\vartheta})(\Lambda \otimes I)\mathbf{R}f\big\|_{L^2(\Omega)} &= \sup_{g \in \mathcal{C}^\infty_0(\Omega)} \frac{|\langle (\mathbf{R}^* - \mathbf{R}^*_{h_\vartheta})\Psi, g\rangle_{L^2}|}{\|g\|_{L^2}} \\ &= \sup_{g \in \mathcal{C}^\infty_0(\Omega)} \frac{\big| \int_0^{2\pi} u(\vartheta)\,\mathrm{d}\vartheta - h_\vartheta \sum_{j=0}^{2p-1} u(jh_\vartheta)\big|}{\|g\|_{L^2}}.\end{aligned}$$

If we are able to bound

$$\int_0^{2\pi} |u^{(2k+1)}(\vartheta)| \mathrm{d}\vartheta \lesssim \|f\|_{2k+1} \|g\|_{L^2}, \quad k \in \mathbb{N}_0, \tag{3.4}$$

we have proved Lemma 3.4 via Lemma 3.3 as well as density and interpolation arguments.

Since

$$\begin{aligned}
\int_0^{2\pi} |u^{(m)}(\vartheta)| \mathrm{d}\vartheta &\leq \int_0^{2\pi}\int_{-1}^{1} \big| D_\vartheta^m \big(\mathbf{R}g(s,\vartheta)\, \Psi(s,\vartheta) \big) \big| \mathrm{d}s \mathrm{d}\vartheta \\
&\leq \sum_{j=0}^{m} \binom{m}{j} \int_0^{2\pi}\int_{-1}^{1} \big| (I \otimes D^{m-j}) \mathbf{R}g(s,\vartheta)\, (\Lambda \otimes D^j) \mathbf{R}f(s,\vartheta) \big| \mathrm{d}s \mathrm{d}\vartheta \\
&\leq \sum_{j=0}^{m} \binom{m}{j} \|(I \otimes D^{m-j}) \mathbf{R}g\|_{H^{(1/2,j-m)}}\, \|(\Lambda \otimes D^j) \mathbf{R}f\|_{H^{(-1/2,m-j)}} \\
&\leq \sum_{j=0}^{m} \binom{m}{j} \|\mathbf{R}g\|_{H^{(1/2,0)}}\, \|\mathbf{R}f\|_{H^{(1/2,m)}} \\
&\overset{(2.9)}{\lesssim} 2^m \|g\|_{L^2}\, \|f\|_m
\end{aligned}$$

estimate (3.4) as well as Lemma 3.4 hold true. □

Now we handle the second error term.

LEMMA 3.5. *Let f be in $H_0^\alpha(\Omega)$. Under the assumptions of Theorem* 3.1 *we have*

$$\big\| (\mathbf{R}^* - \mathbf{R}_{h_\vartheta}^*) \big((\mathrm{I}_h \Lambda E_h - \Lambda) \otimes I \big) \mathbf{R}f \big\|_{L^2(\Omega)} \lesssim h_\vartheta h^{\min\{\alpha_{\max}, \alpha-1\}} \|f\|_\alpha.$$

Proof. We proceed as in the proof of Lemma 3.4. Again we benefit from duality, density and interpolation. Let f and g be in $\mathcal{C}_0^\infty(\Omega)$. Define u as in (3.3), however, with

$$\Psi = \big((\mathrm{I}_h \Lambda E_h - \Lambda) \otimes I \big) \mathbf{R}f.$$

As in the proof of Lemma 3.4 we find that

$$\begin{aligned}
\int_0^{2\pi} |u'(\vartheta)| \mathrm{d}\vartheta &\leq \|(I \otimes D) \mathbf{R}g\|_{H^{(1/2,-1)}} \|\Psi\|_{H^{(-1/2,1)}} \\
&\qquad + \|\mathbf{R}g\|_{H^{(1/2,0)}} \|(I \otimes D)\Psi\|_{H^{(-1/2,0)}} \\
&\leq 2 \|\mathbf{R}g\|_{H^{(1/2,0)}} \|\Psi\|_{H^{(-1/2,1)}} \\
&\lesssim \|g\|_{L^2} \|\Psi\|_{H^{(-1/2,1)}}.
\end{aligned}$$

Further,

$$\begin{aligned}
\|\Psi\|_{H^{(-1/2,1)}} &\le \big\|\big((\mathrm{I}_h\Lambda E_h - \Lambda E_h)\otimes I\big)\mathbf{R}f\big\|_{H^{(-1/2,1)}} \\
&\qquad + \big\|\big((\Lambda E_h - \Lambda)\otimes I\big)\mathbf{R}f\big\|_{H^{(-1/2,1)}} \\
&\overset{(2.7)}{\lesssim} h^{\min\{\alpha_{\mathrm{I}},\alpha-1\}}\|(\Lambda E_h\otimes I)\mathbf{R}f\|_{H^{(\alpha-3/2,1)}} \\
&\qquad + \big\|\big((E_h - I)\otimes I\big)\mathbf{R}f\big\|_{H^{(1/2,1)}} \\
&\overset{(2.6)}{\lesssim} h^{\min\{\alpha_{\mathrm{I}},\alpha-1\}}\|(E_h\otimes I)\mathbf{R}f\|_{H^{(\alpha-1/2,1)}} \\
&\qquad + h^{\min\{\beta_{\max},\alpha-1/2\}-1/2}\|\mathbf{R}f\|_{H^{(\alpha-1/2,1)}} \\
&\overset{(2.6)}{\lesssim} \big(h^{\min\{\alpha_{\mathrm{I}},\tau_{\max}-1/2,\alpha-1\}} + h^{\min\{\beta_{\max}-1/2,\alpha-1\}}\big)\|\mathbf{R}f\|_{H^{(\alpha-1/2,1)}} \\
&\overset{(2.9)}{\lesssim} h^{\min\{\alpha_{\max},\alpha-1\}}\|f\|_{\alpha}.
\end{aligned}$$

Thus,

$$\int_0^{2\pi} |u'(\vartheta)|\mathrm{d}\vartheta \lesssim h^{\min\{\alpha_{\max},\alpha-1\}}\|g\|_{L^2}\|f\|_{\alpha}.$$

Finally,

$$\begin{aligned}
\big\|(\mathbf{R}^* - \mathbf{R}^*_{h_\vartheta})\Psi\big\|_{L^2(\Omega)} &= \sup_{g\in\mathcal{C}_0^\infty(\Omega)} \frac{\big|\int_0^{2\pi} u(\vartheta)\,\mathrm{d}\vartheta - h_\vartheta\sum_{j=0}^{2p-1} u(jh_\vartheta)\big|}{\|g\|_{L^2}} \\
&\lesssim h_\vartheta \sup_{g\in\mathcal{C}_0^\infty(\Omega)} \frac{\int_0^{2\pi}|u'(\vartheta)|\mathrm{d}\vartheta}{\|g\|_{L^2}} \lesssim h_\vartheta h^{\min\{\alpha_{\max},\alpha-1\}}\|f\|_{\alpha}
\end{aligned}$$

ends the proof of Lemma 3.5. □

Now Theorem 3.1 is established by (3.1), Theorem 2.1, (3.2), Lemmas 3.4 and 3.5.

REMARK 3.6. *Unfortunately, our convergence analysis of the FBA does not apply to density distributions appearing in medical imaging. Image densities in medical imaging can be considered elements in* $H_0^\alpha(\Omega)$ *with* $\alpha < 1/2$ *but close to* $1/2$*, see Natterer* [8, pp. 92ff.]*. Theorem* 3.1*, however, requires* $\alpha \ge \alpha_{\min} \ge 1$*. The main reason causing this lower bound on the Sobolev regularity is the error estimate for the composite trapezoidal rule (Lemma* 3.3*). At present we do not know a useful estimate requiring less smoothness of the integrand.*

4. MFBA: a modified filtered backprojection algorithm. In the representation (2.2) of the FBA we see that the Λ-operator is *not* discretized.

Rather, it is applied to the continuous function $(E_h \otimes I)\mathbf{R}f(\cdot, \vartheta_j)$ which interpolates or approximates the discrete Radon data with respect to the lateral variable. We suggest an analogous approach to the angular variable, that is, we interpolate the discrete data with respect to both variables. Now, the Λ-operator and the backprojection operator can act exactly on the resulting continuous bivariate function. We call the resulting numerical scheme *modified filtered backprojection algorithm* (MFBA):

$$\begin{aligned} f_{\mathrm{MFBA}}(x) &:= \frac{1}{4\pi}\mathbf{R}^*(\mathrm{I}_h \otimes I)(\Lambda \otimes I)(E_h \otimes T_{h_\vartheta})\mathbf{R}f(x) \\ &= \frac{1}{4\pi}\mathbf{R}^*(\mathrm{I}_h \Lambda E_h \otimes T_{h_\vartheta})\mathbf{R}f(x) \end{aligned} \tag{4.1}$$

with the periodic linear interpolation

$$T_{h_\vartheta} w(\cdot) = \sum_{j=0}^{2p-1} w(\vartheta_j) C_{h_\vartheta}(\cdot - \vartheta_j)$$

where C_{h_ϑ} is a 2π-*periodized* linear B-spline. More precisely: Let C be the linear B-spline. Then, $C_{h_\vartheta}(\cdot) = \sum_{k\in\mathbb{Z}} C(\cdot/h_\vartheta + 2\pi\, k/h_\vartheta)$.

Before we consider a numerical implementation of MFBA we prove convergence with optimal rates.

4.1. Convergence of MFBA. The key for proving convergence of MFBA is the approximation property

$$\|T_{h_\vartheta} - I\|_{H^\alpha_{\mathrm{p}}(0,2\pi)\to H^{-\nu}_{\mathrm{p}}(0,2\pi)} \lesssim h_\vartheta^{\alpha+\nu}, \qquad 1/2 + \nu < \alpha \le 2, \tag{4.2}$$

for any $0 \le \nu < 1/2$. We will validate (4.2) below in Theorem 4.2.

THEOREM 4.1. *Assume* (2.6) *and* (2.7) *with* $\beta_{\max}, \tau_{\max} \ge 1/2$ *and* $\beta_{\min} < 1$. *Further, let*

$$\mathrm{I}_h : L^2(\mathbb{R}) \to L^2(\mathbb{R}) \quad \textit{be bounded.} \tag{4.3}$$

Then,

$$\Big\| f - \frac{1}{4\pi}\mathbf{R}^*(\mathrm{I}_h \Lambda E_h \otimes T_{h_\vartheta})\mathbf{R}f \Big\|_{L^2(\Omega)} \lesssim \big(h^{\min\{\alpha,\alpha_{\max}\}} + h_\vartheta^{\min\{\alpha,\alpha_{\mathrm{T}}\}}\big)\|f\|_\alpha$$

for $\alpha > \alpha_{\min} = 1/2 + 2\max\{0, \beta_{\min} - 1/2\}$ *where* $\alpha_{\max} = \min\{\alpha_{\mathrm{I}}, \beta_{\max} - 1/2, \tau_{\max} - 1/2\}$ *and any* $\alpha_{\mathrm{T}} < 5/2$.

Proof. We will need that

$$\mathrm{I}_h : H^{-1/2+\nu}(\mathbb{R}) \to H^{-1/2+\nu}(\mathbb{R}) \ \text{ is a bounded operator} \tag{4.4}$$

which follows from (2.7) and (4.3) via interpolation.

We start with

$$\begin{aligned}\big\|f - \frac{1}{4\pi}\mathbf{R}^*(\mathrm{I}_h\Lambda E_h \otimes T_{h_\vartheta})\mathbf{R}f\big\|_{L^2} \\ &\le \big\|f - \frac{1}{4\pi}\mathbf{R}^*(\mathrm{I}_h\Lambda E_h \otimes I)\mathbf{R}f\big\|_{L^2} + \big\|\mathbf{R}^*\big(\mathrm{I}_h\Lambda E_h \otimes (T_{h_\vartheta} - I)\big)\mathbf{R}f\big\|_{L^2} \\ &\lesssim h^{\min\{\alpha,\alpha_{\max}\}}\|f\|_\alpha + \big\|\mathbf{R}^*\big(\mathrm{I}_h\Lambda E_h \otimes (T_{h_\vartheta} - I)\big)\mathbf{R}f\big\|_{L^2},\end{aligned}$$

the last estimate being due to Theorem 2.1. Bounding the remaining error term is basically straightforward. Under $\max\{0, \beta_{\min} - 1/2\} \le \nu < 1/2$ we find that

$$\begin{aligned}\big\|\mathbf{R}^*\big(\mathrm{I}_h\Lambda E_h \otimes (T_{h_\vartheta} - I)\big)\mathbf{R}f\big\|_{L^2} &\overset{(2.9)}{\lesssim} \big\|\big(\mathrm{I}_h\Lambda E_h \otimes (T_{h_\vartheta} - I)\big)\mathbf{R}f\big\|_{H^{(-1/2+\nu,-\nu)}} \\ &\overset{(4.4)}{\lesssim} \big\|\big(\Lambda E_h \otimes (T_{h_\vartheta} - I)\big)\mathbf{R}f\big\|_{H^{(-1/2+\nu,-\nu)}} \\ &\lesssim \big\|\big(E_h \otimes (T_{h_\vartheta} - I)\big)\mathbf{R}f\big\|_{H^{(1/2+\nu,-\nu)}} \\ &\overset{(2.6)}{\lesssim} \big\|\big(I \otimes (T_{h_\vartheta} - I)\big)\mathbf{R}f\big\|_{H^{(1/2+\nu,-\nu)}} \\ &\overset{(4.2)}{\lesssim} h_\vartheta^\alpha\|\mathbf{R}f\|_{H^{(1/2+\nu,\alpha-\nu)}} \overset{(2.9)}{\lesssim} h_\vartheta^\alpha\|f\|_\alpha\end{aligned}$$

where both latter estimates require that $1/2+2\nu < \alpha \le 2+\nu$. Now we have the freedom to choose ν in the admissible range. Choosing $\nu = \alpha_{\mathrm{T}} - 2$ yields $1/2 + 2(\alpha_{\mathrm{T}} - 2) < \alpha \le \alpha_{\mathrm{T}}$. On the other hand, by $\nu = \max\{0, \beta_{\min} - 1/2\}$ we obtain $1/2 + 2\max\{0, \beta_{\min} - 1/2\} < \alpha \le 2 + \max\{0, \beta_{\min} - 1/2\}$. Hence,

$$\big\|\mathbf{R}^*\big(\mathrm{I}_h\Lambda E_h \otimes (T_{h_\vartheta} - I)\big)\mathbf{R}f\big\|_{L^2} \lesssim h_\vartheta^\alpha\|f\|_\alpha$$

for $1/2 + 2\max\{0, \beta_{\min} - 1/2\} < \alpha \le \alpha_{\mathrm{T}} < 5/2$. □

As a consequence of the above theorem the error estimate (1.4) holds true since the corresponding operators I_h satisfy (4.3), see [9] or [11] for more details.

We complete the present section by finally verifying the approximation property (4.2).

THEOREM 4.2. *For any $0 \le \nu < 1/2$ we have that*

$$\|u - T_{h_\vartheta}u\|_{H_{\mathrm{p}}^{-\nu}(0,2\pi)} \lesssim h_\vartheta^{\alpha+\nu}\|u\|_{H_{\mathrm{p}}^{\alpha}(0,2\pi)}, \qquad 1/2 + \nu < \alpha \le 2. \tag{4.5}$$

Proof. We first show the estimate for $\alpha \in [1, 2]$. Let $\varphi_1 \in \mathcal{C}_0^\infty(0, 2\pi)$ and $\varphi_2 \in \mathcal{C}_{\mathrm{p}}^\infty(0, 2\pi)$ with $\tau_\pi\varphi_2 = \varphi_2(\cdot - \pi) \in \mathcal{C}_0^\infty(0, 2\pi)$ such that $\varphi_1 + \varphi_2 = 1 \in$

$\mathcal{C}_{\mathrm{p}}^{\infty}(0,2\pi)$ (partition of unity).** Then,

$$\begin{aligned}\|u - T_{h_\vartheta} u\|_{H_{\mathrm{p}}^{-\nu}(0,2\pi)} &= \|(I - T_{h_\vartheta})(\varphi_1 u + \varphi_2 u)\|_{H_{\mathrm{p}}^{-\nu}(0,2\pi)} \\ &\le \|(I - T_{h_\vartheta})(\varphi_1 u)\|_{H_{\mathrm{p}}^{-\nu}(0,2\pi)} \\ &\qquad + \|(I - T_{h_\vartheta})(\varphi_2 u)\|_{H_{\mathrm{p}}^{-\nu}(0,2\pi)} \\ &\lesssim \|(I - T_{h_\vartheta})(\varphi_1 u)\|_{H_0^{-\nu}(0,2\pi)} \\ &\qquad + \|((I - T_{h_\vartheta})(\varphi_2 u))^*|_{(\pi,3\pi)}\|_{H_0^{-\nu}(\pi,3\pi)},\end{aligned}$$

where w^* denotes the 2π-periodic extension to $\mathbb{R}$ of $w \in H_{\mathrm{p}}^{\beta}(0,2\pi)$, $\beta \in \mathbb{R}$. Suppose we are able to show that

$$\|u - T_{h_\vartheta} u\|_{H_0^{-\nu}(0,2\pi)} \lesssim h_\vartheta^{\alpha+\nu} \|u\|_{H_0^{\alpha}(0,2\pi)}, \qquad 1 \le \alpha \le 2, \tag{4.6}$$

then

$$\begin{aligned}\|u - T_{h_\vartheta} u\|_{H_{\mathrm{p}}^{-\nu}(0,2\pi)} &\lesssim h_\vartheta^{\alpha+\nu} \big(\|\varphi_1 u\|_{H_0^{\alpha}(0,2\pi)} + \|(\varphi_2 u)^*|_{(\pi,3\pi)}\|_{H_0^{\alpha}(\pi,3\pi)} \big) \\ &= h_\vartheta^{\alpha+\nu} \big(\|\varphi_1 u\|_{H_0^{\alpha}(0,2\pi)} + \|\tau_\pi(\varphi_2 u)\|_{H_0^{\alpha}(0,2\pi)} \big) \\ &\lesssim h_\vartheta^{\alpha+\nu} \|u\|_{H_{\mathrm{p}}^{\alpha}(0,2\pi)}, \quad 1 \le \alpha \le 2.\end{aligned}$$

On the other hand, from [9, Theorem A.2] we know that

$$\|u - T_{h_\vartheta} u\|_{L^2(0,2\pi)} \lesssim h_\vartheta^{\alpha} \|u\|_{H_{\mathrm{p}}^{\alpha}(0,2\pi)}, \quad 1/2 < \alpha \le 2.$$

Hence, we are able to deduce (4.5) by an interpolation argument.

Accordingly, we only need to validate (4.6) to establish Theorem 4.2. We begin with the simple triangle inequality

$$\|v - T_{h_\vartheta} v\|_{H_0^{-\nu}(0,2\pi)} \le \|v - \widetilde{T}_{h_\vartheta} v\|_{H_0^{-\nu}(0,2\pi)} + \|\widetilde{T}_{h_\vartheta} v - T_{h_\vartheta} v\|_{H_0^{-\nu}(0,2\pi)} \tag{4.7}$$

where $\widetilde{T}_{h_\vartheta}$ is the following auxiliary approximation operator

$$\widetilde{T}_{h_\vartheta} w := h_\vartheta^{-1} \sum_{j=0}^{2p-1} \langle w, C_{h_\vartheta}(\cdot - \vartheta_j) \rangle \, C_{h_\vartheta}(\cdot - \vartheta_j), \quad w \in L^2(0,2\pi).$$

For the left summand in (4.7) we find that

$$\begin{aligned}\|v - \widetilde{T}_{h_\vartheta} v\|_{H_0^{-\nu}(0,2\pi)} &= \sup_{w \in H^{\nu}(\mathbb{R})} \frac{|\langle v - \widetilde{T}_{h_\vartheta} v, w \rangle|}{\|w\|_{\nu}} = \sup_{w \in H^{\nu}(\mathbb{R})} \frac{|\langle v, w - \widetilde{T}_{h_\vartheta} w \rangle|}{\|w\|_{\nu}} \\ &\le \|v\|_{L^2(0,2\pi)} \sup_{w \in H^{\nu}(\mathbb{R})} \frac{\|w - \widetilde{T}_{h_\vartheta} w\|_{L^2(\mathbb{R})}}{\|w\|_{\nu}} \\ &\lesssim h_\vartheta^{\nu} \|v\|_{L^2(0,2\pi)}\end{aligned} \tag{4.8}$$

**Note that $|||w||| = \|\varphi_1 w\|_{H_0^{\alpha}(0,2\pi)} + \|\tau_\pi(\varphi_2 w)\|_{H_0^{\alpha}(0,2\pi)}$ yields a norm on $H_{\mathrm{p}}^{\alpha}(0,2\pi)$ being equivalent to the standard norm defined via Fourier coefficients, see, e.g., Lions and Magenes [4, Chap. 1.7].

where the last bound is due to [9, Theorem A.2]. We proceed with the right summand of (4.7):

$$\|\widetilde{T}_{h_\vartheta} v - T_{h_\vartheta} v\|_{H_0^{-\nu}(0,2\pi)} = \sup_{w \in H^\nu(\mathbb{R})} \frac{|\langle \widetilde{T}_{h_\vartheta} v - T_{h_\vartheta} v, w\rangle|}{\|w\|_\nu}. \tag{4.9}$$

Since $\widetilde{T}_{h_\vartheta} v - T_{h_\vartheta} v = h_\vartheta^{-1} \sum_{j=0}^{2p-1} \langle v - v(\vartheta_j), C_{h_\vartheta}(\cdot - \vartheta_j)\rangle C_{h_\vartheta}(\cdot - \vartheta_j)$ we have

$$|\langle \widetilde{T}_{h_\vartheta} v - T_{h_\vartheta} v, w\rangle| \le \sum_{j=0}^{2p-1} |\underbrace{\langle v - v(\vartheta_j), h_\vartheta^{-1} C_{h_\vartheta}(\cdot - \vartheta_j)\rangle}_{=: L_j(v)}| \, |\langle C_{h_\vartheta}(\cdot - \vartheta_j), w\rangle|.$$

We next study the linear functional L_j. For $v \in H^1(\vartheta_{j-1}, \vartheta_{j+1})$ we bound

$$|L_j(v)| \le \int_{\vartheta_{j-1}}^{\vartheta_{j+1}} |v(\vartheta) - v(\vartheta_j)| \, h_\vartheta^{-1} C_{h_\vartheta}(\vartheta - \vartheta_j) \, \mathrm{d}\vartheta \le 2\|v\|_{L^\infty(\vartheta_{j-1}, \vartheta_{j+1})}.$$

Further, $L_j(P) = 0$ for any constant P and there is a constant $P = P(v)$ such that the Bramble-Hilbert like estimate

$$\|v - P\|_{L^\infty(\vartheta_{j-1}, \vartheta_{j+1})} \lesssim h_\vartheta^{1/2} \|v\|_{H^1(\vartheta_{j-1}, \vartheta_{j+1})}$$

holds true, see, e.g., Brenner and Scott [2, Proposition 4.3.2]. Combining our findings we have

$$|L_j(v)| = |L_j(v - P)| \lesssim \|v - P\|_{L^\infty(\vartheta_{j-1}, \vartheta_{j+1})} \lesssim h_\vartheta^{1/2} \|v\|_{H^1(\vartheta_{j-1}, \vartheta_{j+1})},$$

so that, for $v \in H_0^1(0, 2\pi)$,

$$\begin{aligned}
&|\langle \widetilde{T}_{h_\vartheta} v - T_{h_\vartheta} v, w\rangle| \\
&\quad \lesssim h_\vartheta^{1/2} \sum_{j=0}^{2p-1} \|v\|_{H^1(\vartheta_{j-1}, \vartheta_{j+1})} \underbrace{\|C_{h_\vartheta}(\cdot - \vartheta_j)|_{[\vartheta_{j-1}, \vartheta_{j+1}]}\|_{-\nu}}_{\lesssim h_\vartheta^{1/2+\nu} \text{ (Lem.4.3 below)}} \|w\|_{H^\nu(\vartheta_{j-1}, \vartheta_{j+1})} \\
&\quad \lesssim h_\vartheta^{1+\nu} \left(\sum_{j=0}^{2p-1} \|v\|^2_{H^1(\vartheta_{j-1}, \vartheta_{j+1})} \right)^{1/2} \left(\sum_{j=0}^{2p-1} \|w\|^2_{H^\nu(\vartheta_{j-1}, \vartheta_{j+1})} \right)^{1/2} \\
&\quad \lesssim h_\vartheta^{1+\nu} \|v\|_1 \|w\|_\nu.
\end{aligned}$$

The latter estimate together with (4.9) results in

$$\|\widetilde{T}_{h_\vartheta} v - T_{h_\vartheta} v\|_{H_0^{-\nu}(0,2\pi)} \lesssim h_\vartheta^{1+\nu} \|v\|_1, \quad v \in H_0^1(0, 2\pi),$$

which in combination with (4.7) and (4.8) implies that

$$\|v - T_{h_\vartheta} v\|_{H_0^{-\nu}(0,2\pi)} \lesssim h_\vartheta^\nu \|v\|_{L^2(0,2\pi)} + h_\vartheta^{1+\nu} \|v\|_1, \quad v \in H_0^1(0, 2\pi).$$

For $u \in H_0^\alpha(0,2\pi)$, $1 \le \alpha \le 2$, set $v := u - T_{h_\vartheta} u \in H_0^1(0,2\pi)$. Note that $v - T_{h_\vartheta} v = u - T_{h_\vartheta} u$. Finally, (4.6) is established by

$$\begin{aligned}\|u - T_{h_\vartheta} u\|_{H_0^{-\nu}(0,2\pi)} &= \|v - T_{h_\vartheta} v\|_{H_0^{-\nu}(0,2\pi)} \lesssim h_\vartheta^\nu \|v\|_{L^2(0,2\pi)} + h_\vartheta^{1+\nu} \|v\|_1 \\ &= h_\vartheta^\nu \|u - T_{h_\vartheta} u\|_{L^2(0,2\pi)} + h_\vartheta^{1+\nu} \|u - T_{h_\vartheta} u\|_1 \\ &\lesssim h_\vartheta^{\alpha+\nu} \, \|u\|_\alpha\end{aligned}$$

where in the last step we once more applied Theorem A.2 of [9]. Thus, Theorem 4.2 is completely verified. □

LEMMA 4.3. *To any $0 \le \nu < 1/2$ there is a constant $c = c(\nu)$ such that*

$$\|C_{h_\vartheta}|_{[h_\vartheta, h_\vartheta]}\|_{-\nu} \le c(\nu)\, h_\vartheta^{1/2+\nu}.$$

Proof. We have

$$\begin{aligned}&\|C_{2h_\vartheta}|_{[2h_\vartheta,2h_\vartheta]}\|_{-\nu}^2 \\ &\quad= \int_{\mathbb{R}} (1+|\sigma|^2)^{-\nu} |\widehat{C_{2h_\vartheta}}(\sigma)|^2 \,\mathrm{d}\sigma = 4h_\vartheta^2 \int_{\mathbb{R}} (1+|\sigma|^2)^{-\nu} |\widehat{C}(2h_\vartheta\sigma)|^2 \,\mathrm{d}\sigma \\ &\quad= 4\sqrt{2\pi} h_\vartheta^2 \int_{\mathbb{R}} (1+|\sigma|^2)^{-\nu} |\mathrm{sinc}^2(h_\vartheta\sigma)|^2 \,\mathrm{d}\sigma \\ &\quad= 4\sqrt{2\pi} h_\vartheta^2 \Bigg(\int_{-h_\vartheta^{-1}}^{h_\vartheta^{-1}} (1+|\sigma|^2)^{-\nu} \underbrace{|\mathrm{sinc}^2(h_\vartheta\sigma)|^2}_{\le 1} \,\mathrm{d}\sigma \\ &\qquad\qquad + \int_{\mathbb{R}\setminus[-h_\vartheta^{-1},h_\vartheta^{-1}]} (1+|\sigma|^2)^{-\nu} \underbrace{|\mathrm{sinc}^2(h_\vartheta\sigma)|^2}_{\le (h_\vartheta\sigma)^{-4}} \,\mathrm{d}\sigma \Bigg) \\ &\quad\le 4\sqrt{2\pi} h_\vartheta^2 \Bigg(\underbrace{\int_{-h_\vartheta^{-1}}^{h_\vartheta^{-1}} |\sigma|^{-2\nu} \,\mathrm{d}\sigma}_{=\frac{2}{1-2\nu} h_\vartheta^{2\nu-1}} + h_\vartheta^{-4} \underbrace{\int_{\mathbb{R}\setminus[-h_\vartheta^{-1},h_\vartheta^{-1}]} |\sigma|^{-2\nu-4} \,\mathrm{d}\sigma}_{=\frac{2}{2\nu+3} h_\vartheta^{2\nu+3}} \Bigg) \\ &\quad= 8\sqrt{2\pi} \left(\frac{1}{1-2\nu} + \frac{1}{2\nu+3} \right) h_\vartheta^{1+2\nu}.\end{aligned}$$

Thus, $c(\nu) = 2^{2-\nu} \sqrt{\sqrt{2\pi}\big(\frac{1}{1-2\nu} + \frac{1}{2\nu+3}\big)}$. □

4.2. Implementation of MFBA. We discuss some aspects concerning the numerical evaluation of $f_{\mathrm{MFBA}}(x)$, see (4.1). Define $\Phi := \frac{1}{4\pi}(\mathrm{I}_h \Lambda E_h \otimes I)\mathbf{R}f$. Then,

$$\Phi(s,\vartheta) = \sum_{k\in\mathbb{Z}} g_k(\vartheta) A_h(s - s_k)$$

where

$$g_k(\vartheta) = \frac{1}{4\pi} h^{-1} \langle (\Lambda E_h \otimes I)\mathbf{R}f(\cdot,\vartheta), \eta_h(\cdot - s_k)\rangle$$

are the filtered Radon data, compare (2.5). We obtain

$$\begin{aligned} f_{\mathrm{MFBA}}(x) &= \frac{1}{4\pi}\mathbf{R}^*(\mathrm{I}_h \Lambda E_h \otimes T_{h_\vartheta})\mathbf{R}f(x) = \int_0^{2\pi} (I \otimes T_{h_\vartheta})\Phi(x^t\omega(\vartheta),\vartheta)\,\mathrm{d}\vartheta \\ &= \int_0^{2\pi} \sum_{j=0}^{2p-1} \Phi(x^t\omega(\vartheta),\vartheta_j) C_{h_\vartheta}(\vartheta - \vartheta_j)\,\mathrm{d}\vartheta \\ &= \int_0^{2\pi} \sum_{j=0}^{2p-1} \sum_{k\in\mathbb{Z}} g_k(\vartheta_j) A_h(x^t\omega(\vartheta) - s_k) C_{h_\vartheta}(\vartheta - \vartheta_j)\,\mathrm{d}\vartheta \\ &= \sum_{k\in\mathbb{Z}} \sum_{j=0}^{2p-1} g_k(\vartheta_j) \int_0^{2\pi} A_h(x^t\omega(\vartheta) - s_k) C_{h_\vartheta}(\vartheta - \vartheta_j)\,\mathrm{d}\vartheta. \end{aligned}$$

Observe that $f_{\mathrm{MFBA}}(0) = f_{\mathrm{FBA}}(0)$.

To reduce the notational burden we introduce the abbreviation

$$I(s,\psi,x) = \int_0^{2\pi} A_h(x^t\omega(\vartheta) - s) C_{h_\vartheta}(\vartheta - \psi)\,\mathrm{d}\vartheta.$$

Since $g_k(\vartheta_j) = g_{-k}(\vartheta_{j+p})$ as well as $I(s_k,\vartheta_j,x) = I(s_{-k},\vartheta_{j+p},x)$ we have that

$$f_{\mathrm{MFBA}}(x) = 2\sum_{k\in\mathbb{Z}} \sum_{j=0}^{p-1} g_k(\vartheta_j) I(s_k,\vartheta_j,x).$$

It remains to compute the integrals $I(s_k,\vartheta_j,x)$. A straightforward calculation gives that ($x \neq 0$)

$$I(s_k,\vartheta_j,x) = I(s_k,\vartheta_j - \arg(x), |x|\omega(0)).^{\dagger\dagger}$$

Thus, we only need to evaluate integrals like

$$I(s_k,\psi,r\omega(0)) = \int_{\psi-h_\vartheta}^{\psi+h_\vartheta} A_h(r\cos(\vartheta) - s_k) C_{h_\vartheta}(\vartheta - \psi)\,\mathrm{d}\vartheta.$$

For $A = \mathbf{1}_{[-1/2,1/2]}$ and $A = \mathbf{1}_{[-1/2,1/2]} \star \mathbf{1}_{[-1/2,1/2]}$ an explicit computation of the above integrals can be found in [11]. Please note that most of the

$^{\dagger\dagger}\arg(x)$ denotes the angle in the polar representation of $x \in \mathbb{R}^2\setminus\{0\}$: $x = |x|\,\omega(\arg(x))$.

integrals are zero and do not need to be computed. For instance, if $A = \mathbf{1}_{[-1/2,1/2]} \star \mathbf{1}_{[-1/2,1/2]}$ then

$$\big[\min\Theta(\psi,h),\max\Theta(\psi,h)\big] \cap \left[\frac{s_{k-1}}{r},\frac{s_{k+1}}{r}\right] = \emptyset \quad\Longrightarrow\quad I(s_k,\psi,r\omega(0)) = 0$$

where $\Theta(\psi,h) = \cos([\psi-h,\psi+h])$.

REMARK 4.4. *In principle, the band matrix $M(x) = \{I(s_k,\vartheta_j,x)\}_{k,j}$ can be precomputed and stored as its entries only depend on the scanning geometry and the reconstruction points where $M(-x)_{k,j} = M(x)_{-k,j}$. Moreover, the bandwidth of M does neither depend on h nor on h_ϑ and it is bounded for $|x| \le 1$. Therefore, MFBA is only slightly more expensive than FBA if the sparse matrices M are precomputed. In our numerical experiments in the following section we however computed the non-zero entries of M on-the-fly.*

5. Numerical illustrations. Numerical experiments illustrating the convergence orders of FBA (Theorem 3.1) under the optimal sampling condition $p = \pi q$ can already be found in [9, Sect. 6]. Further experiments are reported in [11]. We therefore concentrate on experiments highlighting the different convergence behaviors of both algorithms in the lateral and angular variables. Additionally, we compare FBA with MFBA qualitatively.

First we demonstrate that the error term of FBA behaving like h_ϑ^α does indeed not saturate, see (1.2). To this end, we reconstruct a function $f \in H_0^{5/2}(\Omega)$ from discrete data D, see (1.1), with $q = \lfloor p^{5/3} \rfloor$ using the Shepp-Logan filter with piecewise constant interpolation ($\alpha_{\max} = 3/2$). From (1.2) we expect the convergence rate $p^{-5/2}$ as $p \to \infty$.

As density distribution f we use

$$f(x) := \sum_{k=1}^{3} d_k\, P\big(U_k(x-b_k)\big) \tag{5.1}$$

where $P(x) = (1-|x|^2)^{2.01}$, $|x| \le 1$, and $P(x) = 0$, otherwise, and $d_1 = 1$, $d_2 = -1.5$, $d_3 = 1.5$, and $b_1 = (0.22,0)^t$, $b_2 = (-0.22,0)^t$, $b_3 = (0,0.2)^t$. Further, $U_k = U(\varphi_k,\delta_k,\gamma_k)$, $k = 1,2,3$, with

$$U(\varphi,\delta,\gamma) := \begin{pmatrix} \cos(\varphi)/\delta & \sin(\varphi)/\delta \\ -\sin(\varphi)/\gamma & \cos(\varphi)/\gamma \end{pmatrix}$$

and

$$\begin{aligned} &\delta_1 = 0.51, && \gamma_1 = 0.31, && \varphi_1 = 72\pi/180, \\ &\delta_2 = 0.51, && \gamma_2 = 0.36, && \varphi_2 = 108\pi/180, \\ &\delta_3 = 0.5, && \gamma_3 = 0.8, && \varphi_3 = \pi/2. \end{aligned}$$

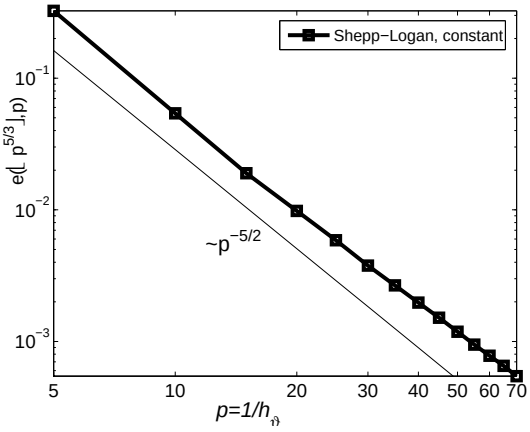

FIG. 5.1. The relative L^2-errors $e\big(\lfloor p^{5/3}\rfloor, p\big)$ (5.2) for reconstructing f (5.1) by FBA using the Shepp-Logan filter with nearest neighbor interpolation. The auxiliary solid line indicates exact decay $p^{-5/2}$.

Note that $f \in H_0^\alpha(\Omega)$ for any $\alpha < 2.51$. For a graphical representation of f see [9, Fig. 2]. The Radon transform of f can be computed analytically. From discrete Radon data we reconstructed

$$f_{\mathrm{FBA,q,p}}(x) = \frac{1}{4\pi}\mathbf{R}^*_{\pi/p}(\mathrm{I}_{1/q}\Lambda E_{1/q} \otimes I)\mathbf{R}f(x), \quad x \in \mathcal{X},$$

on the grid $\mathcal{X} := \Omega \cap \{(i/100, j/100) : -100 \le i, j \le 100\}$. Now we define the relative L^2-reconstruction error by

$$e(q,p) := \Big(\sum_{x\in\mathcal{X}} \big(f_{\mathrm{FBA},q,p}(x) - f(x)\big)^2 \Big/ \sum_{x\in\mathcal{X}} f(x)^2\Big)^{1/2}. \tag{5.2}$$

In Figure 5.1 we plotted $e\big(\lfloor p^{5/3}\rfloor, p\big)$ for $p \in \{5l : l = 1, \ldots, 14\}$. Its decay $\mathrm{O}(q^{-5/2})$ complies exactly with the prediction by (1.2).

Next we illustrate that the convergence order of MFBA in the angular variable may exceed the order in the lateral variable. Let f from (5.1) be reconstructed by

$$f_{\mathrm{MFBA,q,p}}(x) = \frac{1}{4\pi}\mathbf{R}^*(\mathrm{I}_{1/q}\Lambda E_{1/q} \otimes T_{\pi/p})\mathbf{R}f(x), \quad x \in \mathcal{X},$$

with Shepp-Logan filter and nearest neighbor interpolation ($\alpha_{\max} = 3/2$) where $p = \lfloor 3q^{3/5}\rfloor$. In view of (1.4) we expect an error decay rate like $q^{-3/2+\epsilon}$ for any $\epsilon > 0$ which we indeed observe in Figure 5.2.

Finally, we compare both algorithms. We computed relative L^2-errors for the reconstruction of different test objects (e.g. the functions from (5.1) and Figure 5.3) for increasing q and $p = 3q$. It turned out that FBA and MFBA are practically identical in terms of L^2-errors, see Figure 5.6. This

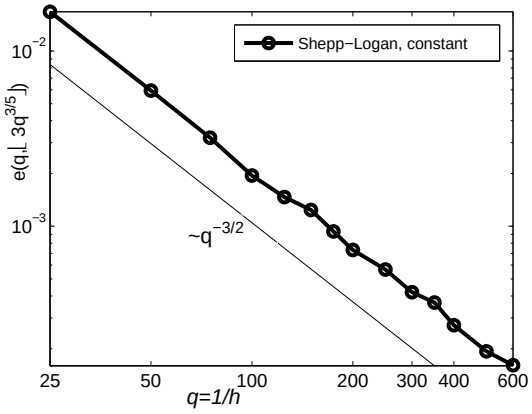

FIG. 5.2. The relative L^2-errors $e\big(q, \lfloor 3q^{3/5} \rfloor\big)$ (5.2) with f from (5.1) and $f_{\mathrm{FBA,q,p}}$ replaced by $f_{\mathrm{MFBA,q,p}}$ (Shepp-Logan filter and nearest neighbor interpolation). The auxiliary solid line indicates exact decay $q^{-3/2}$.

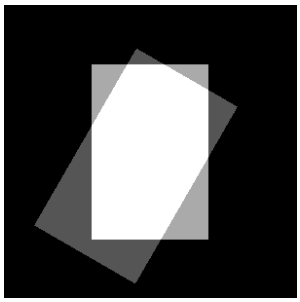

FIG. 5.3. Superposition of indicator functions of two rectangles.

observation remains true when artificial noise corrupts the data. As the L^2-norm is known not to comply well with the human perception of images we inspected reconstructions visually: Near to edges and vertices we found the artifacts of MFBA less pronounced than those of FBA. For a typical example we reconstruct the function displayed in Figure 5.3 being a superposition of indicator functions of two rectangles (For an analytical description see [9, Sec. 6]).

In Figures 5.4 and 5.5 we show close-ups of the reconstructions by FBA and MFBA, respectively. Both reconstructions are based on the Shepp-Logan filter with piecewise linear interpolation where $q = 50$ and $p = 150$. MFBA clearly produces less artefacts which are, moreover, less severe. Accordingly the regions of constant gray values appear more homogeneous, however, at the price of blurred edges.

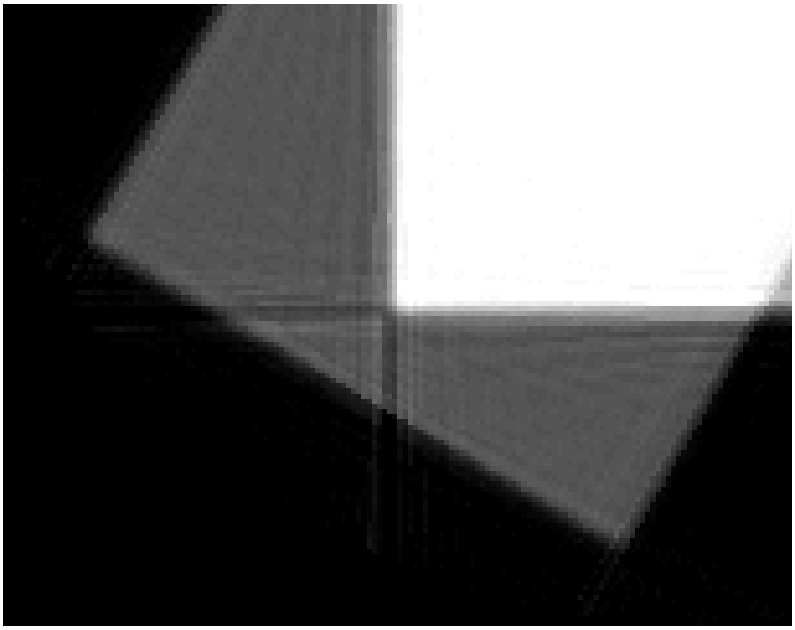

FIG. 5.4. Close-up of the reconstruction by FBA of the function from Figure 5.3 (Shepp-Logan filter, piecewise linear interpolation, $q = 50$, $p = 150$).

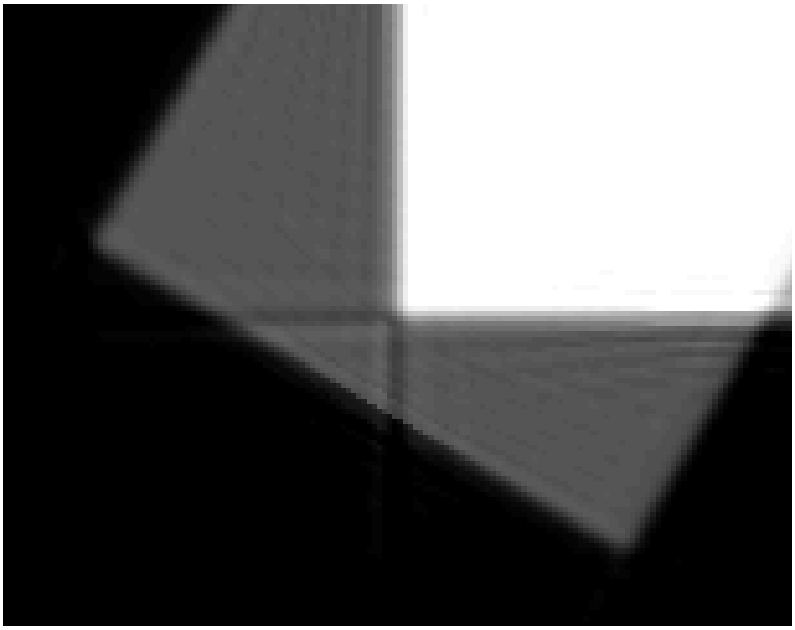

FIG. 5.5. Close-up of the reconstruction by MFBA of the function from Figure 5.3 (Shepp-Logan filter, piecewise linear interpolation, $q = 50$, $p = 150$).

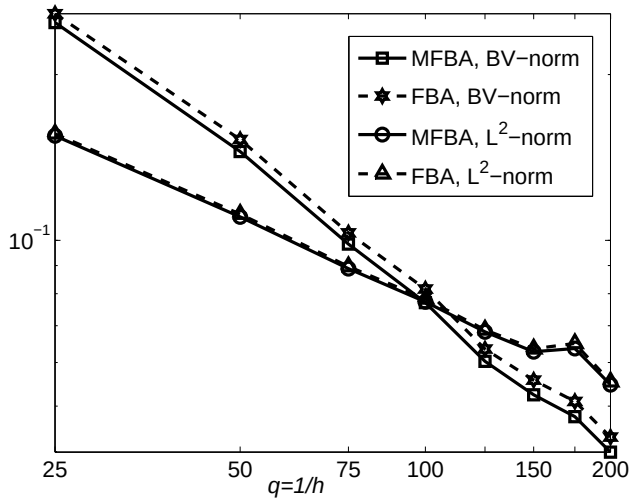

FIG. 5.6. Quantitative comparison of FBA and MFBA with respect to the BV- and L^2-norm. The underlying function is from Figure 5.6. Solid line with $\square$: rel. BV-error of MFBA, solid line with $\circ$: rel. L^2-error of MFBA. Dashed line with $\bigstar$: rel. BV-error of FBA, dashed line with $\triangle$: rel. L^2-error of FBA.

Within the image processing community the norm of bounded variation,

$$\|f\|_{\mathrm{BV}} := \int_\Omega |f(x)|\mathrm{d}x + \int_\Omega |\nabla f|,$$

is considered a measure for comparing images which is almost as sensitive as the human eye: Both, errors in edges and noise, result in a large BV-norm.

Figure 5.6 displays the relative BV- and L^2-errors for reconstructing the function of Figure 5.3 from discrete data where $q \in \{25, 50, 75, 100, 125, 150, 175, 200\}$ and $p = 3q$. Both algorithms, FBA and MFBA, rely on the Shepp-Logan filter with piecewise linear interpolation. While FBA and MFBA produce virtually identical L^2-errors, the corresponding BV-errors differ slightly. MFBA outperforms FBA with respect to both error measures. Interestingly, the BV-errors decay faster than the L^2-errors, roughly like $\mathrm{O}(q^{-3/4})$. So far, we have no analytic explanation for this numerically observed order of decay.

REFERENCES

[1] J.-P. AUBIN, *Applied Functional Analysis*, Pure & Applied Mathematics, Wiley, New York, 2nd ed., 2000.

[2] S. C. BRENNER AND L. R. SCOTT, *The Mathematical Theory of Finite Element Methods*, vol. 15 of Texts in Applied Mathematics, Springer, New York, 1994.

[3] R. KRESS, *Numerical Analysis*, vol. 181 of Graduate Texts in Mathematics, Springer-Verlag, New York, 1998.

[4] J. L. Lions and E. Magenes, *Non-Homogeneous Boundary Value Problems and Applications, Vol.* 1, Springer-Verlag, New York, 1972.

[5] A. K. Louis and F. Natterer, *Mathematical problems in computerized tomography*, Proceedings IEEE, 71 (1983), pp. 379–389.

[6] F. Natterer, *Genauigkeitsfragen bei der numerischen Rekonstruktion von Bildern*, vol. 49 of International series of numerical mathematics (ISNM), Birkhäuser Verlag, Basel, Switzerland, 1979, pp. 131–146.

[7] ———, *A Sobolev space analysis of picture reconstruction*, SIAM J. Appl. Math., 39 (1980), pp. 402–411.

[8] ———, *The Mathematics of Computerized Tomography*, Wiley, Chichester, 1986.

[9] A. Rieder and A. Faridani, *The semi-discrete filtered backprojection algorithm is optimal for tomographic inversion*, SIAM J. Numer. Anal., 41 (2003), pp. 869–892.

[10] A. Rieder and Th. Schuster, *The approximate inverse in action with an application to computerized tomography*, SIAM J. Numer. Anal., 37 (2000), pp. 1909–1929.

[11] A. Schneck, *Konvergenz von Rekonstruktionsalgorithmen in der 2D-Tomographie: Der voll-diskrete Fall (Convergence of reconstruction algorithms in 2D-tomography: The fully discrete case)*. Diploma thesis, Fakultät für Mathematik, Universität Karlsruhe, D-76128 Karlsruhe, Germany, 2006.

[12] L. A. Shepp and B. F. Logan, *The Fourier reconstruction of a head section*, IEEE Trans. Nuc. Sci., 21 (1974), pp. 21–43.

[13] D. T. Smithey, M. Beck, M. G. Raymer, and A. Faridani, *Measurement of the Wigner distribution and the density matrix of a light mode using optical homodyne tomography: Application to squeezed states and the vacuum*, Phys. Rev. Lett., 70 (1993), pp. 1244–1247.

IWRMM-Preprints seit 2004

Nr. 04/01 Andreas Rieder: Inexact Newton Regularization Using Conjugate Gradients as Inner IteractionMichael

Nr. 04/02 Jan Mayer: The ILUCP preconditioner

Nr. 04/03 Andreas Rieder: Runge-Kutta Integrators Yield Optimal Regularization Schemes

Nr. 04/04 Vincent Heuveline: Adaptive Finite Elements for the Steady Free Fall of a Body in a Newtonian Fluid

Nr. 05/01 Götz Alefeld, Zhengyu Wang: Verification of Solutions for Almost Linear Complementarity Problems

Nr. 05/02 Vincent Heuveline, Friedhelm Schieweck: Constrained H^1-interpolation on quadrilateral and hexahedral meshes with hanging nodes

Nr. 05/03 Michael Plum, Christian Wieners: Enclosures for variational inequalities

Nr. 05/04 Jan Mayer: ILUCDP: A Crout ILU Preconditioner with Pivoting and Row Permutation

Nr. 05/05 Reinhard Kirchner, Ulrich Kulisch: Hardware Support for Interval Arithmetic

Nr. 05/06 Jan Mayer: ILUCDP: A Multilevel Crout ILU Preconditioner with Pivoting and Row Permutation

Nr. 06/01 Willy Dörfler, Vincent Heuveline: Convergence of an adaptive *hp* finite element strategy in one dimension

Nr. 06/02 Vincent Heuveline, Hoang Nam-Dung: On two Numerical Approaches for the Boundary Control Stabilization of Semi-linear Parabolic Systems: A Comparison

Nr. 06/03 Andreas Rieder, Armin Lechleiter: Newton Regularizations for Impedance Tomography: A Numerical Study

Nr. 06/04 Götz Alefeld, Xiaojun Chen: A Regularized Projection Method for Complementarity Problems with Non-Lipschitzian Functions

Nr. 06/05 Ulrich Kulisch: Letters to the IEEE Computer Arithmetic Standards Revision Group

Nr. 06/06 Frank Strauss, Vincent Heuveline, Ben Schweizer: Existence and approximation results for shape optimization problems in rotordynamics

Nr. 06/07 Kai Sandfort, Joachim Ohser: Labeling of n-dimensional images with choosable adjacency of the pixels

Nr. 06/08 Jan Mayer: Symmetric Permutations for I-matrices to Delay and Avoid Small Pivots During Factorization

Nr. 06/09 Andreas Rieder, Arne Schneck: Optimality of the fully discrete filtered Backprojection Algorithm for Tomographic Inversion

Nr. 06/10 Patrizio Neff, Krzysztof Chelminski, Wolfgang Müller, Christian Wieners: A numerical solution method for an infinitesimal elasto-plastic Cosserat model

Nr. 06/11 Christian Wieners: Nonlinear solution methods for infinitesimal perfect plasticity

Eine aktuelle Liste aller IWRMM-Preprints finden Sie auf:

www.mathematik.uni-karlsruhe.de/iwrmm/seite/preprints